Accepted Article

MS KATHRIN KÜHNHAMMER (Orcid ID : 0000-0001-5266-2207)

DR MAREN DUBBERT (Orcid ID : 0000-0002-2352-8516)

Article type : Regular Manuscript

Investigating the root plasticity response of *Centaurea jacea* to soil water availability changes from isotopic analysis

Kathrin Kühnhammer[1], Angelika Kübert[2], Nicolas Brüggemann[1], Paulina Deseano Diaz[1], Dagmar van Dusschoten[3], Mathieu Javaux[1,4], Steffen Merz[5], Harry Vereecken[1], Maren Dubbert[2], and Youri Rothfuss[1]

[1]Forschungszentrum Jülich GmbH, Institute of Bio- and Geosciences, Agrosphere Institute (IBG-3), Leo-Brandt-Straße, D-52425 Jülich, Germany

[2]Ecosystem Physiology, University Freiburg, D-79104 Freiburg, Germany

[3]Forschungszentrum Jülich GmbH, Institute of Bio- and Geosciences, Plant Sciences (IBG-2), Leo-Brandt-Straße, D-52425 Jülich, Germany

[4]Earth and Life Institute, Environmental Sciences (ELIE), Université catholique de Louvain (UCL), B-1348 Louvain-la-Neuve, Belgium

[5]Forschungszentrum Jülich GmbH, Institute of Energy and Climate Research, Fundamental Electrochemistry (IEK-9), Leo-Brandt-Straße, D-52425 Jülich, Germany

Author for correspondence:

This article has been accepted for publication and undergone full peer review but has not been through the copyediting, typesetting, pagination and proofreading process, which may lead to differences between this version and the Version of Record. Please cite this article as doi: 10.1111/nph.16352

This article is protected by copyright. All rights reserved

Kathrin Kühnhammer
Tel: +49 (0)761 203 54076
kathrin.kuehnhammer@posteo.de

Youri Rothfuss
Tel: +49 2461 61-96925
y.rothfuss@fz-juelich.de

Received: 4 September 2019

Accepted: 21 November 2019

ORCID

Angelika Kübert: 0000-0003-3985-9261

Dagmar van Dusschoten: 0000-0002-6251-1231

Mathieu Javaux: 0000-0002-6168-5467

Steffen Merz: 0000-0002-2163-5027

Youri Rothfuss: 0000-0002-8874-5036

Harry Vereecken: 0000-0002-8051-8517

Nicholas Brüggemann: 0000-0003-3851-2418

Accepted Article

This article is protected by copyright. All rights reserved

Accepted Article

Summary

- Root water uptake is a key ecohydrological process for which a physically-based understanding has been developed in the past decades. However, due to methodological constraints, knowledge gaps remain about the plastic response of whole plant root systems to a rapidly changing environment.

- We designed a laboratory system for non-destructive monitoring of stable isotopic composition in plant transpiration of an herbaceous species (*Centaurea jacea*) and of soil water across depths, taking advantage of newly developed *in-situ* methods. Daily root water uptake profiles were obtained using a statistical Bayesian multi-source mixing model.

- Fast shifts in the isotopic composition of both soil and transpiration water could be observed with the setup and translated into dynamic and pronounced shifts of the root water uptake profile, even in well-watered conditions.

- The incorporation of plant physiological and soil physical information into statistical modelling improved the model output. A simple exercise of water balance closure underlined the non-unique relationship between root water uptake profile on the one hand, and water content and root distribution profiles on the other, illustrating the continuous adaption of the plant water uptake as a function of its root hydraulic architecture and soil water availability during the experiment

Key words: *Centaurea jacea*, controlled conditions, multi-source Bayesian mixing model, root system plasticity, root water uptake, water stable isotopes

1 Introduction

On a global scale plants might be responsible for returning as much as 80 to 90 % of water from land surfaces to the atmosphere (Jasechko *et al.*, 2013). Consequently, plants have an important influence on climate conditions, i.e. atmospheric moisture content and temperature as well as wind

This article is protected by copyright. All rights reserved

and rainfall patterns on a local to global scale (Sheil, 2014). Root systems impact directly or indirectly soil moisture, soil hydraulic conductivity and thus infiltration and runoff processes (Thompson *et al.*, 2010), which, in turn, influences water resource availability and the occurrence of floods and soil erosion (Schlesinger & Jasechko, 2014; Ola *et al.*, 2015; Dubbert & Werner, 2018). Despite its importance, the magnitude of root water uptake (RWU) and conclusively plant transpiration rate is subject of ongoing debate and associated with high uncertainties (Coenders-Gerrits *et al.*, 2014; Sutanto *et al.*, 2014). This can be attributed to the multiple factors influencing RWU, whose complex and dynamic interactions are currently not thoroughly understood (Rothfuss & Javaux, 2017).

Root water uptake and transport is a passive process driven by the water potential gradient from soil through plants to the atmosphere (Larcher, 2003). Thus, the magnitude and spatial distribution of RWU result on one hand from atmospheric conditions, e.g. vapour pressure deficit (Dubbert *et al.*, 2013; Volkmann *et al.*, 2016a) and from soil water availability (Lobet *et al.*, 2014). On the other hand, plants also respond to heterogeneous hydric conditions by adapting their physiological and morphological properties. The xylem diameter reflects the root segment history. It tends to be smaller for shallow roots exposed to drought or freezing conditions than for deeper roots (Gebauer & Volařík, 2013). Root hydraulic conductivity changes on short time scales in response to nutrient and water availability, even in the course of diurnal cycles (Caldeira *et al.*, 2014). At the leaf level, plants actively regulate the trade-off between CO_2 uptake and excessive water loss through stomatal opening and closing (Blum, 2011). Functional-structural models have demonstrated the impact of such characteristics on the uptake patterns (Couvreur *et al.*, 2014). However, ecological models incorporating RWU generally strongly simplify the aforementioned influencing factors by assuming a direct link between the root density and soil water content profiles with RWU distribution (Varado *et al.*, 2006; Schymanski *et al.*, 2008).

The compositions of oxygen and hydrogen stable isotopes in water differ between ecosystem compartments due to fractionation processes, which make them insightful tracers of water movement (Marshall *et al.*, 2008). It has been shown for a number of plant species that RWU as well as convective transport in xylem vessels induce no measurable isotope fractionation (Wershaw *et al.*, 1966; Dawson *et al.*, 2002). However, for cases where isotope fractionation was observed see e.g. Lin & Sternberg (1993) and Barbeta *et al.* (2019). The isotopic composition of xylem water usually reflects the mixture of RWU and thus across potential soil water sources.

This article is protected by copyright. All rights reserved

When transpiration approaches isotopic steady-state (ISS) under constant micrometeorological conditions, the isotopic composition of transpired water vapour equals that of liquid xylem water (Wang & Yakir, 2000; Dubbert *et al.*, 2017). Therefore, the isotopic method consisting in comparing the isotopic composition of xylem water (or of transpired water vapour at ISS) with those of the plant water sources (i.e., a set of defined layers across the soil profile) was extensively used to identify water uptake patterns and strategies. Studies conducted in a wide range of ecosystems provided insights into, e.g., resource partitioning and competition between plant species (Meinzer *et al.*, 1999), hydraulic lift (Sun *et al.*, 2014; Meunier *et al.*, 2017) as well as rooting depths and depth-dependent uptake dynamics (Beyer *et al.*, 2016). The most common approach for retrieving RWU from isotopic data is the use of multi-source linear mixing models embedded in a Bayesian framework (Parnell *et al.*, 2010). For examples see, e.g., Asbjornsen *et al.* (2007), Prechsl *et al.* (2015), Volkmann *et al.* (2016a). However, to increase the model's predictive power, the soil water isotopic composition profile should (i) show a steep gradient while remaining monotonic and (ii) provide independent information for both monitored isotopes (Rothfuss & Javaux, 2017). Furthermore (iii), only soil water pools identified as plant water sources should be incorporated in the modelling approach, i.e., soil water which is not accessible to the plant for given ecophysiological reasons should be removed from the analysis.

Novel monitoring methods based on laser spectroscopy and gas-permeable membranes allow for a non-destructive determination of the isotopic composition of soil water (Rothfuss *et al.*, 2013, 2015; Volkmann & Weiler, 2014; Oerter *et al.*, 2017) and of tree xylem water (Volkmann *et al.*, 2016b). They overcome a number of limitations associated with destructive sampling of soil and plant material and subsequent extraction of water in the laboratory for isotopic analysis (Orlowski *et al.*, 2016a) and noticeably increase the temporal resolution of collected data. The possibility to measure water vapour continuously also allows for directly determining the isotopic composition of the transpiration flux (Wang *et al.*, 2012; Dubbert *et al.*, 2014).

The present study's central objective was to investigate from non-destructive isotopic measurements the temporal dynamics of root plasticity response to changes of water availability. We will make quantitative observations of the link between soil water availability (via the proxy of soil water content), root length density and RWU distribution.

For this we (i) developed a full soil-plant atmosphere isotopic monitoring experimental setup (diagram of the setup in Supporting Information, Fig. S1) based on the combination of laser

This article is protected by copyright. All rights reserved

spectroscopy, gas-permeable tubing for sampling of the soil gas phase, and a plant transpiration chamber (see, e.g., Dubbert *et al.*, 2014) and we (ii) chose *Centaurea jacea*, a perennial herbaceous species well-adapted to drought conditions. We (iii) used a multi-step labeling approach to enhance the vertical gradient of soil water isotopic composition, while mimicking naturally varying boundary conditions, e.g., due to precipitation and rise of the groundwater level. We (iv) ran the Bayesian multi-source mixing model Stable Isotope Analysis in R (SIAR, Parnell *et al.*, 2010) by taking into account additional (non-isotopic) information to retrieve RWU profiles, which we finally confronted to observations of soil water content and root distribution vertical profiles.

Accepted Article

This article is protected by copyright. All rights reserved

2 Material and Methods

The hydrogen and oxygen isotopic compositions of water (δ^2H and $\delta^{18}O$) are reported in per mil (‰) on the international "delta" scale as defined by Gonfiantini (1978). Isotopic measurements were performed with a cavity ring-down spectroscopy (CRDS) analyzer (L2130-i, Picarro, Santa Clara, CA, USA).

Measurement of the soil column and standards

RWU of *Centaurea jacea* was investigated using the experimental design of Rothfuss *et al*. (2015). An acrylic glass column (i.d. = 11 cm, height = 60 cm, volume = 5.7 l) was equipped at 1, 3, 5, 7, 10, 20, 40 and 60 cm depth with microporous polypropylene tubing (length: 17.5 cm, Accurel® PP V8/2 HF, Membrana GmbH, Germany) positioned horizontally. The column was filled with dry soil (silt loam, particle size distribution: 38 % 2-0.063 mm, 48 % 0.063-0.002 mm, 14 % <0.002 mm, dry bulk density: 1.11 g cm^{-3}, porosity: 0.52 cm^3 cm^{-3}) and saturated from the bottom with deionized water ($\delta^{18}O$ = -8.0 ± 0.1 ‰, δ^2H = -53.6 ± 0.9 ‰) on 14 November 2017. The bare soil column was then allowed to evaporate in the laboratory until plant transplantation.

The experimental setup allowed for sampling water vapour in thermodynamic equilibrium with soil liquid water twice a day for 30 min at each soil depth. For this, 50 ml min^{-1} of dry synthetic air (20.5% O_2, 79.5% N_2, Air Liquide, Germany) was directed into the permeable tubing. In addition, the sampled soil water vapour was diluted with 30 ml min^{-1} dry synthetic air close to the outlet of each sampling depth to prevent vapour condensation inside the sample lines.

For each individual measurement that showed a stable plateau and standard deviations (SD) smaller than 0.35 ‰ and 0.9 ‰ for $\delta^{18}O$ and δ^2H, respectively, the soil water vapour raw isotopic compositions and mixing ratio were averaged over the last 600 data points (approximately 10 min). Considering thermodynamic equilibrium between liquid and gaseous water, the isotopic composition of liquid soil water (δ_{soil}) was calculated from that of the sampled water vapour using the temperature-dependent empirical calibration equations of Rothfuss *et al*. (2013). For this, soil temperature (T_S, °C) was recorded at 3, 10, 40 and 60 cm depth with thermocouples (type K, Greisinger electronic GmbH, Regenstauf, Germany, precision: 0.01 °C). The analyzer-specific dependency of isotopic readings on volumetric water vapour mixing ratio (w) values was accounted for (Schmidt *et al.*, 2010). δ_{soil} raw values were corrected at w = 15 000 ppmv. These

This article is protected by copyright. All rights reserved

values were standardized against those of two water vapour standards. For this, two acrylic glass standard vessels, as described by Rothfuss *et al.*, (2013) were equipped with polypropylene tubing, filled with the same silty-loam soil, saturated from the bottom with two isotopically distinct waters (S_{light}: $\delta^{18}O$ = -19.7 ± 0.2 ‰, $\delta^{2}H$ = -83.2 ± 0.5 ‰, and S_{heavy}: $\delta^{18}O$ = 16.9 ± 0.1 ‰, $\delta^{2}H$ = 35.1 ± 0.6 ‰) and placed in an insulated box where temperature was monitored. Standards were each measured four times throughout the day. Finally, standardized δ_{soil} values were linearly interpolated in time (at 17:00 h) to obtain daily δ_{soil} profiles.

Plant measurements

To combine measurements of isotopic compositions in soil water and plant transpiration, the whole aboveground part of the plant was enclosed in a transparent plant chamber (volume = 22.6 l), equipped with a set of five fans ensuring mixing of the air and a sensor monitoring chamber air relative humidity (RH) and temperature (T_a) (RFT-2, METER Group, Munich, Germany, precision: RH 2%, T_a 0.1°C). The chamber air was not in contact with the soil surface, and the chamber walls were coated with FEP foil (4PTFE, Stuhr, Germany) to minimize isotopic exchange (Dubbert *et al.*, 2014). Ambient laboratory air was run through the plant chamber at a flow rate between 1.7 l min^{-1} and 4.5 l min^{-1}, depending on soil water availability and plant development. The water vapour mixing ratio of ambient laboratory air (w_{in}) and its isotopic composition (δ_{in}) were determined before and after each chamber measurement by sampling the air provided to the plant chamber. Values were linearly interpolated in time to obtain one value at the time chamber air outflow was sampled. Chamber air outflow water vapour mixing ratio (w_{out}) and isotopic composition (δ_{out}) were measured three times each day for one hour with measurements ending at 12:00 h, 17:45 h and 23:30 h. The isotopic composition of the transpired water vapour (δ_T) was calculated using Eqn. 1 (Simonin *et al.*, 2013; Dubbert *et al.*, 2014).

$$\delta_T = \frac{w_{out}\delta_{out} - w_{in}\delta_{in}}{w_{out} - w_{in}} - \frac{w_{in}w_{out}(\delta_{out} - \delta_{in})}{w_{out} - w_{in}} \quad (1)$$

Note that, as for δ_{soil} measurements, δ_{in} and δ_{out} were corrected for dependency of the laser spectrometer readings to w and further standardized. Transpiration rate (T in mol m^{-2} s^{-1}) was calculated considering mass conservation with the molar flow rate into the chamber (Eqn. 2, u in mol s^{-1}, calculated from chamber air inflow in l min^{-1} assuming a molar volume of 22.41 l mol^{-1}) (Von Caemmerer & Farquhar, 1981) and scaled to the column's cross-sectional area

This article is protected by copyright. All rights reserved

(A=0.0095 m^2). As in Eqn 1, increased air flow out of the chamber in consequence of addition of water by T is corrected for using $u\,(1 - w_{in}) = u_{out}\,(1 - w_{out})$.

$$T = \frac{u}{A}\frac{(w_{out} - w_{in})}{(1 - w_{out})} \quad (2)$$

Vapour pressure deficit (VPD, in kPa) was computed from values of RH and T_a (Murray, 1966). At the end of the experiment, roots were destructively collected from the soil column at 1, 3, 5, 7, 10, 20, 40 and 60 cm depth and analysed for length density (RLD, in cm root cm^{-3} soil) with the software WinRhizo® (Regent Instruments Inc., Québec, Canada).

Manipulation of soil column water status and isotopic composition

One *Centaurea jacea* individual was transplanted in the soil column in a predrilled hole of 17 cm depth. It was provided with a light source (V600 Reflector Series, VIPARSPECTRA, China; 16h light, 8h dark) automatically switched on daily at 09:15 h. The plants leaf area increased roughly from 30 cm² on DoE 1 to 80 cm² on DoE 20, after which it remained constant. To reduce evaporation from the soil surface, the column was covered. After transplantation and from day of experiment – DoE – 1 to 3, the soil was irrigated with isotopically enriched water (W_{heavy}: 30 ml d^{-1}, $\delta^{18}O$ = 9.6 ± 0.1 ‰, $\delta^{2}H$ = 6.4 ± 0.2 ‰) from the top. From DoE 7 to 10, isotopically depleted water (W_{light}: 125 ml d^{-1}, $\delta^{18}O$ = -18.7 ± 0.0 ‰, $\delta^{2}H$ = -80.0 ± 0.3 ‰) was added from the bottom. The volume and isotopic composition of the water introduced to the soil column provided the prerequisite for retrieving RWU profiles from stable isotope analysis. It increased both soil water $\delta^{18}O$ and $\delta^{2}H$ depth gradients while keeping the decrease of soil water $\delta^{18}O$ and $\delta^{2}H$ monotonic with depth. Importantly, the isotopically labelled water was not added at defined depths in the soil column (as in Moreira *et al.*, (2000); Stahl *et al.* (2013) and Beyer *et al.* (2016)) as the objective was to mimic naturally varying boundary conditions, e.g., due to precipitation and rise of the groundwater level. From DoE 35 to 38 irrigation from the top was repeated using the same isotopically enriched water as after transplantation while increasing the amount added (150 ml d^{-1}). This should simulate a second rain event and give insight into RWU plasticity with a more developed root system.

Soil volumetric water content (θ, m^3 m^{-3}) was recorded at 1, 10, 20, 40 and 60 cm depth with frequency domain sensors (EC-5, Decagon Devices, USA, precision 0.02 m^3 m^{-3}). Soil water matric potential (Ψ, MPa) was calculated from θ and the retention curve parameters: residual water

This article is protected by copyright. All rights reserved

content (θ_r), saturated water content (θ_{sat}) and the shape parameters α and n (Van Genuchten, 1980). The values of θ_r (0.02 $cm^3\ cm^{-3}$), θ_{sat} (0.59 $cm^3\ cm^{-3}$), α (0.022 cm^{-1}) and n (1.22) were determined using a laboratory evaporation method (HYPROP, METER Group, Munich, Germany) (Peters & Durner, 2008) for the silt-loam soil at bulk density of the soil column.

For commodity, in the following the experiment is split into three time phases, delimited by the consecutive isotopic labelling pulses: DoE 1-6 (phase I), DoE 7-34 (phase II) and DoE 35-48 (phase III).

Statistical analysis

All values are reported as mean with their corresponding SD. Building on the approach developed by Phillips & Gregg (2001), the SD of processed data was calculated by means of error propagation using Taylor series applied in every step of data processing. Hereby, uncertainties of all variables were assumed to be independent (compare also Braud *et al.* (2009) and Rothfuss *et al.* (2010)). On average calculated SD for $\delta^{18}O$ and $\delta^{2}H$ were 0.4 ‰ and 1.0 ‰ as well as 0.8 ‰ and 2.0 ‰ for soil and transpiration measurements, respectively.

Linear regressions between $\delta^{18}O$ and $\delta^{2}H$ for soil liquid water (evaporation line, EL) were compared to those calculated for δ_T during the different phases of the experiment. The intrusion of isotopically depleted ambient air water vapour in the upper three cm of soil shifted the soil liquid isotopic composition away from the soil evaporation line in a dual plot. Therefore, linear regressions for the top and bottom of the soil column were calculated separately. Data processing and statistical analysis were conducted with R, version 3.4.3 (R Core Team, 2017).

Modelling root water uptake with a statistical multi-source mixing model

The contributions of the different sources (defined as soil water from the eight monitored layers 0-2, 2-4, 4-6, 6-8.5, 8.5-15, 15-30, 30-50, and 50-60 cm) to RWU were estimated on the basis of δ_{soil} and δ_T and by using the multi-source Bayesian inference mixing model Stable Isotope Analysis in R (SIAR, Parnell *et al.*, 2010). For this, we assumed that transpiration was at ISS (δ_T equals that of the xylem water, i.e., that of RWU). SIAR allows for incorporating the uncertainty in source but not in target (i.e., transpired water vapour) isotopic composition measurements. To cope with this limitation, each δ_T measurement entered the calculation as a group of three values, representing

This article is protected by copyright. All rights reserved

the mean isotopic composition as well as the mean plus and minus the calculated SD (i.e., from error propagation).

The first δ_T measurement of each experimental day (2.5 h after lights were switched on) often showed systematic deviations from the other two, which is related to a violation of the steady-state assumption (Dubbert *et al.*, 2014). To verify this, we estimated the leaf water turnover term τ (Song *et al.*, 2015, Eqn. 3) with W, leaf water content in mol m^{-2} and w_i, saturated water vapour concentration at chamber air temperature.

$$\tau = \frac{W}{T}\left(1 - \frac{w_{in}}{w_i}\right) \quad (3)$$

For this calculation we used a generous assumption of the plants leaf area (100 cm^2) instead of scaling T to the column's cross-sectional area. With a mean value of W = 10.1 mol m^{-2} determined for the investigated species, the mean value for τ was 1.0 ± 0.4 (range: 0.5-2.9 h). Chamber conditions were stable from 12:00 on. Assuming, it took 3 x τ for ISS to be reached (Förstel, 1978), the second and third daily transpiration measurements (i.e., corresponding to 5.75 and 11.5 h of stable conditions, respectively) should have been close to ISS, exception being for the second measurement on DoE 34 with τ = 2.9 h (all other days $\tau \leq 1.8$ h). We did however not exclude the latter data point because its isotopic composition did not markedly differ from that of the following measurement.

Daily RWU fractions (f_{RWU}, -) were modelled using the mean isotopic composition from measurements two and three only. Neglecting the time lag arising from water transport in the plant, corresponding soil profiles were interpolated at 20:30 h, centred between δ_T values two and three. In a field study, a minimum leaf water potential of -3.5 ± 0.5 MPa was measured in July (peak drought) for the investigated species (data not shown). A value of -4 MPa was chosen as threshold below which soil water was considered not available to this particular plant, and the respective soil water source depths were excluded from the SIAR simulations.

At each time step, the model output consisted of 10 000 possible combinations of source fractions. From this output, the most frequent value (mfv, -) of each source fraction was determined on the basis of 1 % increments. The best run, defined as the combination of source fractions minimizing the root mean square error (RMSE) of the set of mfv across all depths, was then derived. The best run has the advantage over the set of mfv to sum up to 1 and therefore close the water balance. To

This article is protected by copyright. All rights reserved

enable the interpretation of spatial patterns, in figures we account for the heterogeneous distribution of soil water probes across the soil column. Therefore, modelled RWU fractions were standardized to the respective soil volumes to obtain values of the RWU fraction per cm soil depth.

Investigating the temporal dynamics of root plasticity response to changes of water availability

In a first step we checked for water balance closure at the column scale. For this we verified if the difference of water head computed between inputs (i.e., addition of water from the top/ bottom of the soil column) and output (i.e., transpiration losses) reflected the changes of water head indicated by the soil water content sensors. Water head is herein expressed in litre of water per unit of column surface area (in m^2) which yields therefore to mm water.

In a second step, we compared for each observation time and across the column depths how well daily changes of soil water content (defined as $\Delta\theta/\Delta t$ and expressed in m^3 water m^{-3} soil d^{-1}, with t the time variable) matched the simulated RWU obtained with SIAR. RWU quantifies here the volume of water extracted daily by the plant from a given soil layer of volume V_{soil}, is defined as the negative product $-f_{RWU} \times T/V_{soil}$, and is also expressed in m^3 water m^{-3} soil d^{-1}. In between irrigation events, where soil water redistribution (e.g. by drainage and capillary rise) is much lower in absolute value than RWU, the temporal changes of soil water content should be almost solely due to RWU.

In a third step, we further selected three days where these conditions were met and compared the RWU profiles with soil water content and root length distribution profiles in order to observe the prevalence of the mechanism of root water compensation and, in general, of the ecological concept of root plasticity to changes of soil water availability.

This article is protected by copyright. All rights reserved

3 Results and Discussion

In-situ isotopic measurements of soil water and transpired water vapour

The addition of water to the top and bottom of the column resulted in pronounced changes of θ, $\delta^{18}O$, and $\delta^{2}H$ along the soil profile. Figure 1 shows profiles in daily time resolution. Above the soil profiles, corresponding daily values of δ_T are also provided. While below 20 cm depth δ_{soil} still reflected the isotopic composition of the water used for the initial saturation of the column during phase I, saturation from the bottom of the column created a strong isotopic decrease with increasing depth during phase II. During the latter phase, the aim of obtaining isotopically distinguishable soil depths was achieved. θ at 40 and 60 cm depth increased strongly during saturation. However, at 40 cm depth this was not accompanied by a comparable change in δ_{soil}, suggesting that antecedent soil water was pushed upwards by newly added water. This should have resulted in a sharp isotopic front (Gazis & Feng, 2004), which was not observed due to limited spatial resolution. The missing instantaneous change of δ_{soil} at 60 cm depth on DoE 7 can be attributed to the time lag needed for new water to replace old water in the micropores of the polypropylene tubing (Rothfuss *et al.*, 2013). After saturation, capillary rise first led to a decrease of δ_{soil} at 40 cm depth. This effect was observed at all soil depths above 60 cm from DoE 12 onwards. Progressively, isotopic diffusion reduced the artificial δ_{soil} gradients as also illustrated by the increase of δ_{soil} at 60 cm depth (DoE 17 to 48). Irrigation at the beginning of phase III led to an increase in θ and δ_{soil} in the first 20 cm of the soil column. The strong initial isotopic enrichment at 20 cm (DoE 35-38) points toward a preferential flow component during water infiltration. Here, the predrilled hole for transplanting *Centaurea jacea*, that also featured soil compaction along its walls and at its bottom likely resulted in higher permeability of the upper soil layers. Over the course of phase III evaporative enrichment dominated the development of δ_{soil} in the columns top 10 cm. On DoE 35 values in 1 cm soil depth were close to those of irrigation water with 5.3 ‰ and 6.1 ‰, at the end of phase III (DoE 48), values were 19.0 ‰ and 43.7 ‰ for $\delta^{18}O$ and $\delta^{2}H$, respectively.

Figure 2 displays the time series of Ψ across soil depths, VPD of the plant chamber atmosphere along with T and δ_T. The difference of isotopic response of *Centaurea jacea* to the addition of water from the bottom (phase II) and the second irrigation from the top (phase III) reflected the difference of plant development and capacity to extract water from the soil. While T (respectively

This article is protected by copyright. All rights reserved

δ_T) gradually increased (decreased) from DoE 3 onward, an increase of δ_T in the order of +20 ‰ and +57 ‰ for $\delta^{18}O$ and $\delta^{2}H$, respectively, was observed after DoE 35. In contrast, T did not change abruptly, but progressively with increasing θ of the upper soil layers. The highest value of T was observed one day after irrigation in phase III was ceased. Only for the beginning of phase II the decrease in δ_T translated into clear changes in the modelled RWU pattern. The simultaneous evolution of δ_{soil} due to the redistribution of water across the soil profile provides an explanation. This highlights the necessity for monitoring both δ_T and δ_{soil} with high time resolution, when investigating the dynamics of RWU patterns with water stable isotopes.

VPD followed a clear diurnal pattern and decreased to a constant value around 1 kPa. In line with the change of VPD, δ_{out} increased as a result of increased contribution from leaf transpired water vapour after LED lights were switched on. A systematic isotopic enrichment of the first compared to the subsequent two transpiration measurements of each day was clearly observable for $\delta^{18}O$. This cannot explicitly be related to diurnal variations in RWU, which was observed by e.g. Doussan *et al.* (2006). Instead, it is likely that higher δ-values arose from a violation of the steady-state assumption. This seems contradictory to recent studies. During daytime, Lai *et al.* (2006) and Dubbert *et al.* (2013, 2014) observed a decrease of δ_T compared to transpiration steady-state values. The increase of VPD was identified as underlying cause. In the present experiment, however, VPD was lower during the photoperiod in contrast to a typical diurnal cycle under field conditions. Dubbert *et al.* (2017) investigated isotopic adjustment of transpiration of different species in response to an abrupt decrease in VPD, which led to an immediate increase in $\delta^{18}O$ and a subsequent, species-specific return to the isotopic composition of source water. Therefore, determination of the time for adjustment of investigated species in relation to the fluctuations of their environmental conditions is needed not only under natural conditions, but also in the context of laboratory experiments. Next to VPD, also a change of δ_{out} impacts the isotopic composition of leaf water and therefore δ_T (Farquhar & Cernusak, 2005). An increase of δ_{out} would however result in a decrease of δ_T. As the opposite was observed, it can be concluded that the change of VPD outweighs the δ_{out} effect in the present experiment.

Soil water and transpiration isotopic data in the dual isotope space

The comparison of δ_{soil} and δ_T in a dual isotope coordinate system allows for identifying the water pools contributing to RWU (Fig. 3). For ease of understanding, experimental phase II (DoE 7-34)

This article is protected by copyright. All rights reserved

was divided into two periods separated by the data gap, i.e., phase II.1 (DoE 7-18 and phase II.2 (DoE 23-34).

Slopes of the $\delta^{18}O$-$\delta^{2}H$ linear regressions for soil depth > 3 cm decreased over time from 3.61 (phase I) to 2.82 (phase III). Slopes of the transpiration lines were similar to those of the EL (for soil depth > 3 cm) and spanned between 2.57 in phase III and 3.52 in phase II.1. Influence of ambient water vapour on δ_{soil} at 1 and 3 cm depth shifted soil water $\delta^{18}O$ and $\delta^{2}H$ values away from the EL in a similar spatial pattern as observed by Rothfuss *et al.* (2015). Consequently, values of δ_{soil} were enclosed in a narrow, two-dimensional polygon (displayed in Fig. 3 in light grey). Nevertheless, soil water $\delta^{18}O$ and $\delta^{2}H$ were linearly correlated during the whole course of the experiment (minimal R^2=0.96 in phase II.2, p-value<$2.2e^{-16}$) due to active capillary rise and isotopic diffusion. Thus, the aim of obtaining independent information from $\delta^{18}O$ and $\delta^{2}H$ was only partly fulfilled. In future experiments, this problem should be addressed, e.g. by adding tracers with different $\delta^{2}H$-to-$\delta^{18}O$ ratios to the soil profile.

δ_T plotted inside the area spanned by δ_{soil} during experimental phases II and III. This accordance indicates that δ_{soil} reflected water pools available for RWU for a wide range of Ψ. Additionally, δ_{soil} below 20 cm depth and deionized water used for initial saturation agreed well before phase II. Therefore, no measurable tension- and texture-mediated isotopic effect (Orlowski *et al.*, 2013, 2016b; Gaj *et al.*, 2017) was found in this study. For the soil used in the present experiment, this also contradicts the recently controversially discussed hypothesis of two water worlds (McDonnell, 2014) that explains observed differences between plant and stream water isotopic compositions by conceptualizing the co-existence of two isotopically distinct water pools, one available for RWU, and one available for soil water flow. Comparably, no isotopic distinction of soil water into 'mobile' and 'immobile' fractions was found by Sprenger *et al.* (2016) and McCutcheon *et al.* (2017).

Simulated RWU profiles and comparison to changes of soil water content

Figure 4 displays the evolution of modelled RWU profiles (f_{RWU} is the dimensionless fraction of root water uptake). For this visual display we standardized modelled values to uptake per cm soil depth to account for different soil layer volumes and enable the interpretation of spatial patterns. As a reference point, the time spans when water was added to the profile are indicated by dashed white lines. Table 1 reports modelled f_{RWU} of the SIAR best run for the eight measured soil depths

This article is protected by copyright. All rights reserved

with the associated ranges. Despite the wide range of potential contributing fractions across water sources, i.e., soil layers, of the model output (Table 1), clear f_{RWU} patterns were found.

Figure 5 shows the observed water head daily changes (in mm d^{-1}), as inferred from (i) the temporal changes of θ (x-axis) and from (ii) the sum of transpiration and irrigation amounts (y-axis). In between irrigation events, a good correspondence (RMSE=0.7 mm d^{-1}, blue symbols) was obtained between the two independent methods, meaning that the setup could properly catch the water dynamics at the column scale. However, at certain days (DoE 1-3, 7-13, and 35-38, red symbols), differences were observed, e.g. due to the spatial resolution of the θ sensors.

Figure 6 shows the depth profiles of RWU (defined as the negative product $-f_{RWU} \times T/V_{soil}$, see Material and Methods section, a) and of the temporal changes in θ ($\Delta\theta/\Delta t$, b), both expressed in m^3 water m^{-3} soil d^{-1}. As no efflux from the roots was simulated by SIAR, it remained negative throughout the experiment. $\Delta\theta/\Delta t$ is the sum (soil water redistribution + RWU) and was observed to be either negative or positive. When $\Delta\theta/\Delta t > 0$, more water was brought to the soil layer by (re)distribution of moisture (e.g., by capillary flow or hydraulic lift) than lost by RWU. This happened on irrigation days, e.g., from DoE 7-10 (respectively DoE 35-38) between 30-60 cm (down to 30 cm depth). Interestingly, on DoE 39 an increase of θ was recorded in 50-60 cm depth which could point to either preferential flow, enhanced by the development of the root system (e.g. Ghestem *et al.*, 2011), or redistribution of moisture by the roots (e.g. Meunier *et al.*, 2017) from shallower, wetter layers (Ψ>-0.1 MPa) to the deeper and much drier bottom soil layer (Ψ<-10 MPa). On DoE 26, 29, and 48, the difference of water volumes lost by the soil column derived from the two methods was smallest, specifically lower than 2 % of transpiration. On these specific days, there was an overall significant linear correlation (R^2=0.45, p-value<0.01) between profiles of water head (in mm d^{-1}) (Fig. 7a). Nevertheless, discrepancies between soil water content temporal change and RWU arose at given soil layers. This is particularly visible at 1 cm depth on DoE 26 and 29, where RWU was always significant even though θ was low (θ<0.16 m^3 m^{-3}, Ψ<-2.7 MPa Fig. 7b). Concurrently, almost no change in θ was recorded. On the opposite, from 30-60 cm depth, changes of θ were always higher than the simulated RWU.

Ecohydrological interpretation of simulated RWU

In the beginning of the experiment, especially during DoE 1-3 when the column was irrigated from the top, RWU mainly occurred in the soil column's top 6 cm and f_{RWU} decreased with soil

This article is protected by copyright. All rights reserved

depth. As water was available to the plant in the entire soil profile, this presumptively reflected the RLD profile (Draye *et al.*, 2010), which typically shows an exponential shape in vertically homogeneous soils (Gregory, 2006). However, a change in the uptake pattern towards a more evenly distributed uptake was observed immediately after irrigation was stopped, when Ψ at 1 and 10 cm decreased, but were still well above field capacity (DoE 1: Ψ_{1cm} = -0.1 MPa, Ψ_{10cm} = -0.3 MPa, DoE 6: Ψ_{1cm} = -0.3 MPa, Ψ_{10cm} = -0.4 MPa). This indicates that RWU could be more sensitive towards changes in Ψ and less associated with RLD than previously assumed. Accordingly, no unique relationship between RWU and RLD profiles (Fig. 7c) was found. These results contradict ecohydrological models that usually assume a strong connection between RWU and the RLD profile, only incorporating information on Ψ when soil water is strongly limited (Feddes *et al.*, 2001; Varado *et al.*, 2006; Schymanski *et al.*, 2008).

Simulated RWU deeper in the soil profile increased during experimental phase II. Here, the cumulated f_{RWU} for 30-60 cm depth (sum of the two soil water layers with measurements in 40 and 60 cm depth) consistently exceeded 45 % for DoEs 10-27. Plants often optimize their root growth to prevailing environmental conditions in order to maximize the use of available resources (Topp, 2016; Rothfuss & Javaux, 2017). This directional growth of the root system, also known as root plasticity, could have been induced by the increasing difference of θ across the soil profile in reaction to the saturation from the bottom.

Even though δ_T and associated RWU profiles changed, T stayed constant for most of phase II, which highlights the prevalence of the compensation mechanism, meaning RWU is relocated to soil regions where water is less tightly bound (Šimůnek & Hopmans, 2009). This mechanism drives RWU in case of spatially heterogeneous water availability (Couvreur *et al.*, 2012). In the present experiment, VPD inside the plant chamber stayed on a constant level following the step change after lights were switched on. This indicates that T was often limited by the ambient conditions and not by soil water availability. Thus, under field conditions that usually feature a faster removal of water vapour from air surrounding the leaf, T could presumably change more dynamically in reaction to changes in the RWU pattern.

From DoE 30 until the end of phase II, water availability became a limiting factor and thus T decreased (compare Fig. 2a and 2b). Consequently, an increasing number of soil layers were excluded from modelling as contributing soil water sources (compare Fig. 4). On DoE 34, we restricted the modelled RWU to 20 and 40 cm soil depth only. This clearly affected modelling

This article is protected by copyright. All rights reserved

results compared to the purely statistical approach, i.e., without restricting soil water sources (see Fig. S2). In the latter approach, RWU increased in the soil top (0-8.5 cm) from DoE 30 until the end of phase II, which contrasted with low Ψ in these soil depths. Analogously, on DoE 34, the highest f_{RWU} (24 %) was simulated for the soil layer 50-60 cm, even though it had the lowest Ψ (-13 MPa). Because plants usually show a minimal water potential (-3.5 MPa for the investigated species) to avoid xylem cavitation that ultimately leads to hydraulic failure (Maherali *et al.*, 2004), this result disagrees with plant physiological concepts. Accordingly, setting f_{RWU}=0 for layer 0-2 cm (30-60 cm) on DoE 29 (respectively DoE 48) noticeably improved the correlation between profiles of water head in comparison to the RWU model without restriction (R^2=0.26, p-value<0.1). This highlights difficulties associated with purely statistical RWU models and illustrates the need for accounting for plant physiological knowledge in simulations (Mahindawansha *et al.*, 2018). An incorporation of actual, dynamic values for Ψ_{plant} instead of a minimum threshold value likely further increases the disagreement between purely statistical and restricted RWU model.

The plant showed an immediate reaction to the irrigation from the top in phase III, when it entirely shifted its RWU to 0-8.5 cm. Directly after water addition, RWU was especially high at 1 and 3 cm depth, despite the fact that soil water was available to the plant at least in the top 20 cm. Together with the fast change of T and RWU location, this could illustrate a strategy of the drought-adapted *Centaurea jacea* to efficiently use as much as possible of, e.g., short but intense summer rains before water becomes limiting again and thus entail a competitive advantage.

Even though the RLD profile certainly changed throughout the experiment, variations in the physical rooting system cannot provide a complete explanation for temporal shifts in the RWU profile due to the velocity of observed changes. In general, RWU seemed to be preferentially associated with water availability rather than with RLD, as also concluded by Kulmatiski *et al.* (2017). This again is visible at the end of the experiment where the simulated decrease of f_{RWU} in 1-6 cm depth is in line with the pronounced decrease of θ at these depths. If and to what extent observed disagreements between RWU and θ profiles arise from uncertainties in the modelling approach or an insufficient understanding of RWU dynamics and the complex interplay of its underlying mechanisms cannot be answered conclusively. This highlights the necessity for the development and validation of process-based modelling approaches (Meunier *et al.*, 2017; Rothfuss & Javaux, 2017).

This article is protected by copyright. All rights reserved

4 Conclusion

We successfully combined *in-situ* methods quantifying the stable isotopic composition in plant transpiration and across soil water sources in the laboratory during a multi-step labelling experiment. Overcoming previous limitations, the combination between plant and soil isotopic datasets allowed for modelling RWU profiles at high temporal resolution. There was no unique relationship between RWU, θ and RLD profiles, illustrating that the plant continuously adapted its uptake distribution as a function of its root hydraulic architecture and soil water availability. Nevertheless, it can be concluded that trends in RWU patterns did overall match better with water availability across the soil profile than with RLD distribution. Furthermore, RWU could be even more dynamic in reaction to Ψ than previously assumed. Even on days when water balances (from daily transpiration and changes of θ) matched well, water head profiles from both independent methods differed. We therefore conclude that using changes in θ as a proxy for RWU (MacFall *et al.*, 1991) or hydraulic redistribution (Domec *et al.*, 2010) leads to biases arising from the simultaneous water redistribution by the soil matrix and/or through plant roots as also observed in a modelling study conducted by Vandoorne *et al.* (2012).

To increase the explanatory power of statistical mixing models, efforts should be directed at further (artificially) decorrelating the δ^2H-$\delta^{18}O$ linear relationship in soil water, thus diversifying information derived from both monitored water stable isotopic signatures. The present work illustrated also the potential to elaborate statistical RWU models by including mechanistic knowledge, i.e., plant and soil physical and physiological information. This approach should be further developed in future studies. Obtained datasets could be used for validating hypotheses made in mechanistic modelling approaches. Possible applications range from implicit models with high computational speed (Couvreur *et al.*, 2012) to models incorporating 3D root systems, root development and the influence of highly resolved soil properties in space and time (Javaux *et al.*, 2008).

This article is protected by copyright. All rights reserved

Accepted Article

5 Acknowledgements

The authors would like to thank Andreas Lücke, Lutz Weihermüller, and Holger Wissel for their scientific and technical support. The present work was conducted within the framework of the DFG-funded research program "Assessing ecohydrological responses from single plant to community scale using a stable isotope approach" (RO-5421-1 and DU-1688/1-1).

6 Author Contribution

NB, MD, and YR planned and designed the experiment. KK, DvD, PDD, SM, and YR conducted the experiment. KK collected the laboratory data and wrote the manuscript. AK collected the field data for parametrization of the statistical model. KK, MJ and YR analysed the data. AK, DvD, MD, NB, and HV helped with data interpretation. All authors reviewed the manuscript.

This article is protected by copyright. All rights reserved

7 References

Asbjornsen H, Mora G, Helmers MJ. **2007**. Variation in water uptake dynamics among contrasting agricultural and native plant communities in the Midwestern U.S. *Agriculture, Ecosystems & Environment* **121**: 343–356.

Barbeta A, Jones SP, Clavé L, Wingate L, Gimeno TE, Fréjaville B, Wohl S, Ogée J. **2019**. Unexplained hydrogen isotope offsets complicate the identification and quantification of tree water sources in a riparian forest. *Hydrology and Earth System Sciences* **23**: 2129–2146.

Beyer M, Koeniger P, Gaj M, Hamutoko JT, Wanke H, Himmelsbach T. **2016**. A deuterium-based labeling technique for the investigation of rooting depths, water uptake dynamics and unsaturated zone water transport in semiarid environments. *Journal of Hydrology* **533**: 627–643.

Blum A. **2011**. Plant breeding for water-limited environments. New York, US: Springer Science+Business Media.

Braud I, Biron P, Bariac T, Richard P, Canale L, Gaudet JP, Vauclin M. **2009**. Isotopic composition of bare soil evaporated water vapor. Part I: RUBIC IV experimental setup and results. *Journal of Hydrology* **369**: 1–16.

Von Caemmerer S, Farquhar GD. **1981**. Some relationships between the biochemistry of photosynthesis and the gas exchange of leaves. *Planta* **153**: 376–387.

Caldeira CF, Jeanguenin L, Chaumont F, Tardieu F. **2014**. Circadian rhythms of hydraulic conductance and growth are enhanced by drought and improve plant performance. *Nature Communications* **5**: 5365.

Coenders-Gerrits AMJ, der Ent RJ, Bogaard TA, Wang-Erlandsson L, Hrachowitz M, Savenije HHG. **2014**. Uncertainties in transpiration estimates. *Nature* **506**: E1.

Couvreur V, Vanderborght J, Draye X, Javaux M. **2014**. Dynamic aspects of soil water availability for isohydric plants: focus on root hydraulic resistances. *Water Resources Research* **50**: 8891–8906.

Couvreur V, Vanderborght J, Javaux M. **2012**. A simple three-dimensional macroscopic root water uptake model based on the hydraulic architecture approach. *Hydrology and Earth System*

This article is protected by copyright. All rights reserved

Sciences **16**: 2957–2971.

Dawson TE, Mambelli S, Plamboeck AH, Templer PH, Tu KP. **2002**. Stable isotopes in plant ecology. *Annual Review of Ecology and Systematics* **33**: 507–559.

Domec J-C, King JS, Noormets A, Treasure E, Gavazzi MJ, Sun G, McNulty SG. **2010**. Hydraulic redistribution of soil water by roots affects whole-stand evapotranspiration and net ecosystem carbon exchange. *New Phytologist* **187**: 171–183.

Doussan C, Pierret A, Garrigues E, Pagès L. **2006**. Water uptake by plant roots: II modelling of water transfer in the soil root-system with explicit account of flow within the root system - comparison with experiments. *Plant and Soil* **283**: 99–117.

Draye X, Kim Y, Lobet G, Javaux M. **2010**. Model-assisted integration of physiological and environmental constraints affecting the dynamic and spatial patterns of root water uptake from soils. *Journal of Experimental Botany* **61**: 2145–2155.

Dubbert M, Cuntz M, Piayda A, Maguás C, Werner C. **2013**. Partitioning evapotranspiration - Testing the Craig and Gordon model with field measurements of oxygen isotope ratios of evaporative fluxes. *Journal of Hydrology* **496**: 142–153.

Dubbert M, Cuntz M, Piayda A, Werner C. **2014**. Oxygen isotope signatures of transpired water vapor: the role of isotopic non-steady-state transpiration under natural conditions. *New Phytologist* **203**: 1242–1252.

Dubbert M, Kübert A, Werner C. **2017**. Impact of leaf traits on temporal dynamics of transpired oxygen isotope signatures and its impact on atmospheric vapor. *Frontiers in Plant Science* **8**. doi: 10.3389/fpls.2017.00005.

Dubbert M, Werner C. **2018**. Water fluxes mediated by vegetation: emerging isotopic insights at the soil and atmosphere interfaces. *New Phytologist* **221**: 1754-1763.

Farquhar GD, Cernusak LA. **2005**. On the isotopic composition of leaf water in the non-steady state. *Functional Plant Biology* **32**: 293.

Feddes RA, Hoff H, Bruen M, Dawson T, de Rosnay P, Dirmeyer P, Jackson RB, Kabat P, Kleidon A, Lilly A, *et al.* 2001. Modeling root water uptake in hydrological and climate models. *Bulletin of the American Meteorological Society* **82**: 2797–2809.

This article is protected by copyright. All rights reserved

Förstel H. **1978**. The enrichment of ^{18}O in leaf water under natural conditions. *Radiation and Environmental Biophysics* **15**: 323–344.

Gaj M, Kaufhold S, Koeniger P, Beyer M, Weiler M, Himmelsbach T. **2017**. Mineral mediated isotope fractionation of soil water. *Rapid Communications in Mass Spectrometry* **31**: 269–280.

Gazis C, Feng X. **2004**. A stable isotope study of soil water: Evidence for mixing and preferential flow paths. *Geoderma* **119**: 97–111.

Gebauer R, Volařík D. **2013**. Root hydraulic conductivity and vessel structure modification with increasing soil depth of two oak species: *Quercus pubescens* and *Quercus robur*. *Trees* **27**: 523–531.

Van Genuchten MT. **1980**. A closed-form equation for predicting the hydraulic properties of unsaturated soils. *Soil Science Society of America Journal* **44**: 892–898.

Ghestem M, Sidle RC, Stokes A. **2011**. The influence of plant root systems on subsurface flow: implications for slope stability. *BioScience* **61**: 869–879.

Gonfiantini R. **1978**. Standards for stable isotope measurements in natural compounds. *Nature* **271**: 534–536.

Gregory PJ. **2006**. Roots, rhizosphere and soil: the route to a better understanding of soil science? *European Journal of Soil Science* **57**: 2–12.

Jasechko S, Sharp ZD, Gibson JJ, Birks SJ, Yi Y, Fawcett PJ. **2013**. Terrestrial water fluxes dominated by transpiration. *Nature* **496**: 347–351.

Javaux M, Schröder T, Vanderborght J, Vereecken H. **2008**. Use of a three-dimensional detailed modeling approach for predicting root water uptake. *Vadose Zone Journal* **7**: 1079–1088.

Kulmatiski A, Adler PB, Stark JM, Tredennick AT. **2017**. Water and nitrogen uptake are better associated with resource availability than root biomass. *Ecosphere* **8**: e01738.

Lai C-T, Ehleringer JR, Bond BJ, Tha Paw U K. **2006**. Contributions of evaporation, isotopic non-steady state transpiration and atmospheric mixing on the $\delta^{18}O$ of water vapour in Pacific Northwest coniferous forests. *Plant, Cell & Environment* **29**: 77–94.

This article is protected by copyright. All rights reserved

Larcher W. **2003**. Physiological plant ecology: ecophysiology and stress physiology of functional groups. Berlin Heidelberg, Germany: Springer Verlag.

Lin G, Sternberg L da S. **1993**. Hydrogen isotopic fractionation by plant roots during water uptake in coastal wetland plants. In: Ehleringer JR, Hall AE, Farquhar GD, eds. *Stable isotopes and plant carbon-water relations*. Academic Press, 497–510.

Lobet G, Couvreur V, Meunier F, Javaux M, Draye X. **2014**. Plant water uptake in drying soils. *Plant Physiology* **164**: 1619–1627.

MacFall JS, Johnson GA, Kramer PJ. **1991**. Comparative water uptake by roots of different ages in seedlings of Loblolly pine (*Pinus taeda L.*). *New Phytologist* **119**: 551–560.

Maherali H, Pockman WT, Jackson RB. **2004**. Adaptive variations in the vulnerability of woody plants to xylem cavitation. *Ecology* **85**: 2184–2199.

Mahindawansha A, Orlowski N, Kraft P, Rothfuss Y, Racela H, Breuer L. **2018**. Quantification of plant water uptake by water stable isotopes in rice paddy systems. *Plant and Soil* **429**: 281–302.

Marshall JD, Brooks JR, Lajtha K. **2008**. Sources of variation in the stable isotopic composition of plants. In: Michener R, Lajtha K: *Stable isotopes in ecology and environmental science*. Oxford, UK: Blackwell Publishing Ltd, 22–60.

McCutcheon RJ, McNamara JP, Kohn MJ, Evans SL. **2017**. An evaluation of the ecohydrological separation hypothesis in a semiarid catchment. *Hydrological Processes* **31**: 783–799.

McDonnell JJ. **2014**. The two water worlds hypothesis: ecohydrological separation of water between streams and trees? *Wiley Interdisciplinary Reviews: Water* **1**: 323–329.

Meinzer FC, Andrade JL, Goldstein G, Holbrook NM, Cavelier J, Wright SJ. **1999**. Partitioning of soil water among canopy trees in a seasonally dry tropical forest. *Oecologia* **121**: 293–301.

Meunier F, Rothfuss Y, Bariac T, Biron P, Richard P, Durand J-L, Couvreur V, Vanderborght J, Javaux M. **2017**. Measuring and modeling hydraulic lift of *Lolium multiflorum* using stable water isotopes. *Vadose Zone Journal* **17**. doi:10.2136/vzj2016.12.0134.

This article is protected by copyright. All rights reserved

Moreira MZ, Sternberg L da SL, Nepstad DC. **2000**. Vertical patterns of soil water uptake by plants in a primary forest and an abandoned pasture in the eastern Amazon: an isotopic approach. *Plant and Soil* **222**: 95–107.

Murray FW. **1966**. *On the computation of saturation vapor pressure.* (No. P-3423). Rand Corp Santa Monica Calif

Oerter EJ, Perelet A, Pardyjak E, Bowen G. **2017**. Membrane inlet laser spectroscopy to measure H and O stable isotope compositions of soil and sediment pore water with high sample throughput. *Rapid Communications in Mass Spectrometry* **31**: 75–84.

Ola A, Dodd IC, Quinton JN. **2015**. Can we manipulate root system architecture to control soil erosion? *SOIL* **1**: 603–612.

Orlowski N, Breuer L, McDonnell JJ. **2016a**. Critical issues with cryogenic extraction of soil water for stable isotope analysis. *Ecohydrology* **9**: 1–5.

Orlowski N, Frede H-G, Brüggemann N, Breuer L. **2013**. Validation and application of a cryogenic vacuum extraction system for soil and plant water extraction for isotope analysis. *Journal of Sensors and Sensor Systems* **2**: 179–193.

Orlowski N, Pratt DL, McDonnell JJ. **2016b**. Intercomparison of soil pore water extraction methods for stable isotope analysis. *Hydrological Processes* **30**: 3434–3449.

Parnell AC, Inger R, Bearhop S, Jackson AL. **2010**. Source partitioning using stable isotopes: coping with too much variation. *PloS one* **5**: e9672.

Peters A, Durner W. **2008**. Simplified evaporation method for determining soil hydraulic properties. *Journal of Hydrology* **356**: 147–162.

Phillips DL, Gregg JW. **2001**. Uncertainty in source partitioning using stable isotopes. *Oecologia* **127**: 171–179.

Prechsl UE, Burri S, Gilgen AK, Kahmen A, Buchmann N. **2015**. No shift to a deeper water uptake depth in response to summer drought of two lowland and sub-alpine C3-grasslands in Switzerland. *Oecologia* **177**: 97–111.

R Core Team. **2018**. R: A language and environment for statistical computing. R version 3.5.2, R Foundation for Statistical Computing, https://www.r-project.org/

This article is protected by copyright. All rights reserved

Rothfuss Y, Biron P, Braud I, Canale L, Durand J-L, Gaudet J-P, Richard P, Vauclin M, Bariac T. **2010**. Partitioning evapotranspiration fluxes into soil evaporation and plant transpiration using water stable isotopes under controlled conditions. *Hydrological Processes* **24**: 3177–3194.

Rothfuss Y, Javaux M. **2017**. Reviews and syntheses: Isotopic approaches to quantify root water uptake: a review and comparison of methods. *Biogeosciences* **14**: 2199–2224.

Rothfuss Y, Merz S, Vanderborght J, Hermes N, Weuthen A, Pohlmeier A, Vereecken H, Brüggemann N. **2015**. Long-term and high-frequency non-destructive monitoring of water stable isotope profiles in an evaporating soil column. *Hydrology and Earth System Sciences* **19**: 4067–4080.

Rothfuss Y, Vereecken H, Brüggemann N. **2013**. Monitoring water stable isotopic composition in soils using gas-permeable tubing and infrared laser absorption spectroscopy. *Water Resources Research* **49**: 3747–3755.

Schlesinger WH, Jasechko S. **2014**. Transpiration in the global water cycle. *Agricultural and Forest Meteorology* **189--190**: 115–117.

Schmidt M, Maseyk K, Lett C, Biron P, Richard P, Bariac T, Seibt U. **2010**. Concentration effects on laser-based $\delta^{18}O$ and $\delta^{2}H$ measurements and implications for the calibration of vapour measurements with liquid standards. *Rapid Communications in Mass Spectrometry* **24**: 3553–3561.

Schymanski SJ, Sivapalan M, Roderick ML, Beringer J, Hutley LB. **2008**. An optimality-based model of the coupled soil moisture and root dynamics. *Hydrology and Earth System Sciences* **12**: 913–932.

Sheil D. **2014**. How plants water our planet: advances and imperatives. *Trends in Plant Science* **19**: 209–211.

Simonin KA, Roddy AB, Link P, Apodaca R, Tu KP, Hu JIA, Dawson TE, Barbour MM. **2013**. Isotopic composition of transpiration and rates of change in leaf water isotopologue storage in response to environmental variables. *Plant, Cell & Environment* **36**: 2190–2206.

Šimůnek J, Hopmans JW. **2009**. Modeling compensated root water and nutrient uptake. *Ecological Modelling* **220**: 505–521.

This article is protected by copyright. All rights reserved

Song X, Simonin KA, Loucos KE, Barbour MM. **2015**. Modelling non-steady-state isotope enrichment of leaf water in a gas-exchange cuvette environment. *Plant, Cell & Environment* **38**: 2618–2628.

Sprenger M, Leistert H, Gimbel K, Weiler M. **2016**. Illuminating hydrological processes at the soil-vegetation-atmosphere interface with water stable isotopes. *Reviews of Geophysics* **54**: 674–704.

Stahl C, Hérault B, Rossi V, Burban B, Bréchet C, Bonal D. **2013**. Depth of soil water uptake by tropical rainforest trees during dry periods: does tree dimension matter? *Oecologia* **173**: 1191–1201.

Sun S-J, Meng P, Zhang J-S, Wan X. **2014**. Hydraulic lift by *Juglans regia* relates to nutrient status in the intercropped shallow-root crop plant. *Plant and Soil* **374**: 629–641.

Sutanto SJ, van den Hurk B, Dirmeyer PA, Seneviratne SI, Röckmann T, Trenberth KE, Blyth EM, Wenninger J, Hoffmann G. **2014**. HESS Opinions: A perspective on isotope versus non-isotope approaches to determine the contribution of transpiration to total evaporation. *Hydrology and Earth System Sciences* **18**: 2815–2827.

Thompson SE, Harman CJ, Heine P, Katul GG. **2010**. Vegetation-infiltration relationships across climatic and soil type gradients. *Journal of Geophysical Research: Biogeosciences* **115**. doi:10.1029/2009JG001134.

Topp CN. **2016**. Hope in change: the role of root plasticity in crop yield stability. *Plant Physiology* **172**: 5–6.

Vandoorne B, Beff L, Lutts S, Javaux M. **2012**. Root water uptake dynamics of *Cichorium intybus* var. *sativum* under water-limited conditions. *Vadose Zone Journal* **11**. doi:10.2136/vzj2012.0005.

Varado N, Braud I, Ross PJ. **2006**. Development and assessment of an efficient vadose zone module solving the 1D Richards' equation and including root extraction by plants. *Journal of Hydrology* **323**: 258–275.

Volkmann THM, Haberer K, Gessler A, Weiler M. **2016a**. High-resolution isotope measurements resolve rapid ecohydrological dynamics at the soil--plant interface. *New Phytologist*

This article is protected by copyright. All rights reserved

210: 839–849.

Volkmann THM, Kühnhammer K, Herbstritt B, Gessler A, Weiler M. **2016b**. A method for in situ monitoring of the isotope composition of tree xylem water using laser spectroscopy. *Plant, Cell & Environment* **39**: 2055–2063.

Volkmann THM, Weiler M. **2014**. Continual in situ monitoring of pore water stable isotopes in the subsurface. *Hydrology and Earth System Sciences* **18**: 1819–1833.

Wang L, Good SP, Caylor KK, Cernusak LA. **2012**. Direct quantification of leaf transpiration isotopic composition. *Agricultural and Forest Meteorology* **154**: 127–135.

Wang X-F, Yakir D. **2000**. Using stable isotopes of water in evapotranspiration studies. *Hydrological Processes* **14**: 1407–1421.

Wershaw RL, Friedman I, Heller SJ, Frank PA. **1966**. Hydrogen isotopic fractionation of water passing through trees. *Advances in Organic Geochemistry*: 55–67.

Accepted Article

This article is protected by copyright. All rights reserved

Accepted Article

8 Figures

Figure 1

Fig. 1: Soil isotopic composition and water content as profiles over depth and time. Also displayed are daily mean isotope values in plant transpiration of Centaurea jacea (δ_T). The time series was divided into phases indicating the addition of isotopically distinct water. In phase I (a-c) the column was irrigated from the top with water enriched in heavy isotopes on Day of Experiment (DoE) 1-3 (30 ml d^{-1}, $\delta^{18}O$ = 9.6 ± 0.1 ‰, $\delta^{2}H$ = 6.4 ± 0.2 ‰), on DoE 7-10 in phase II (d-f) the column bottom was saturated with depleted water (125 ml d-1, $\delta^{18}O$ = -18.7 ± 0.0 ‰, $\delta^{2}H$ = -80.0 ± 0.3 ‰). The column was again irrigated from the top on DoE 35-48 in phase III (g-i) with the same water used in phase I but with increased amount (150 ml d-1). Dashed lines show the isotopic composition of water used for initial full saturation of the soil column. Mean standard deviation for all soil measurements were 0.4 ‰ and 1.0 ‰ for $\delta^{18}O$ and $\delta^{2}H$, respectively.

Figure 2

Fig. 2: Timeline of the isotopic composition of transpired water vapour (δ_T) as mean values with standard deviations (c). Also provided are transpiration rate (T) with vapour pressure deficit (VPD) in the plant chamber (b) and water potentials (Ψ) in different soil depths (a, logarithmic y-axis). As a reference, the minimum water potential (MWP) for the investigated species Centaurea jacea (Ψ_{plant} = -4 MPa) is displayed as a dashed line. Grey shaded areas indicate times when water was added to the soil column. From Day of Experiment (DoE) 18 to 22 transpiration measurements had to be discarded due to condensation inside the tubing.

Figure 3

Fig. 3: Isotopic composition in soil profiles and transpiration of Centaurea jacea (δ_T) in the dual isotope space. Data was divided into the experimental phases with different water input: a) phase I, addition of water from the top, b,c) phase II, addition of water from the bottom, d) addition of water from the top. Crosses indicate the standard deviation of data points as applied in the modelling approach. The isotopic composition of water added to the soil column over the course of the experiment from the top (W_{heavy}) and from the bottom (W_{light}) is also provided. Dashed lines show linear regressions through soil measurements at the column top (depth 1-3 cm) and the column bottom (5-60 cm), solid lines represent linear regressions through transpiration data. For comparison, the blue solid line shows the Global Meteoric Water Line (GMWL). Grey shaded areas drawn for phases II and III illustrate the possible spread of δ_T values.

This article is protected by copyright. All rights reserved

Figure 4

Fig. 4: Temporal evolution of root water uptake fractions of Centaurea jacea (f_{RWU}) simulated by the multi-source mixing model SIAR for each of the eight considered soil layers (0-2, 2-4, 4-6, 6-8.5, 8.5-15, 15-30, 30-50, and 50-60 cm). Values were further normalized by the thickness of each layer and expressed in cm^{-1}. Soil layers coloured in black indicate their exclusion as potential sources for water uptake (f_{RWU}= 0 for soil water potential ≤ -4 MPa) before running SIAR. Start- and endpoints of time spans when water was actively added to the column are indicated by dashed lines.

Figure 5

Fig. 5: Comparison between the volumes of water head daily changes (converted into height of water and expressed in mm d^{-1}) by the soil column as derived from the changes of soil water content (x-axis) and from measured transpiration fluxes of Centaurea jacea and amount of water applied during irrigation events (y-axis).

Figure 6

Fig. 6: Comparison between depth profiles of (a) root water uptake of Centaurea jacea (RWU, defined as the negative product $-f_{RWU} \times T/V_{soil}$) and (b) daily changes of soil water content ($\Delta\theta/\Delta t$), both expressed in m^3 water m^{-3} soil d^{-1}. RWU remained negative throughout the experiment, as no efflux from roots was simulated by SIAR. $\Delta\theta/\Delta t$ is the sum (soil water redistribution + RWU) and was observed to be either negative or positive.

Figure 7

Fig. 7: Water head daily changes (in mm d^{-1}) across soil layers as determined from the changes of soil water content (referred to as "water balance") and from the multi-source mixing model ("isotopic balance") on day of experiment (DoE) 26, 29 and 48 (a). Also displayed are the corresponding soil water content (θ, in m^3 m^{-3}) profiles (b) and the root length density (RLD, in cm cm^{-3}) profile of the investigated species Centaurea jacea measured destructively at the end of the experimental period (c).

This article is protected by copyright. All rights reserved

9 Tables

Table 1: Modelled root water uptake fractions for the investigated species Centaurea jacea per day of experiment (DoE) for each soil water source in % as best runs with associated ranges. From DoE 18 to 22 transpiration measurements had to be discarded due to condensation inside the tubing. Values on these days are displayed as not available (NA).

Accepted Article

This article is protected by copyright. All rights reserved

Accepted Article

10 Supporting Information

Additional supporting information may be found in the online version of this article.

Fig. S1 Schematic of the experimental setup

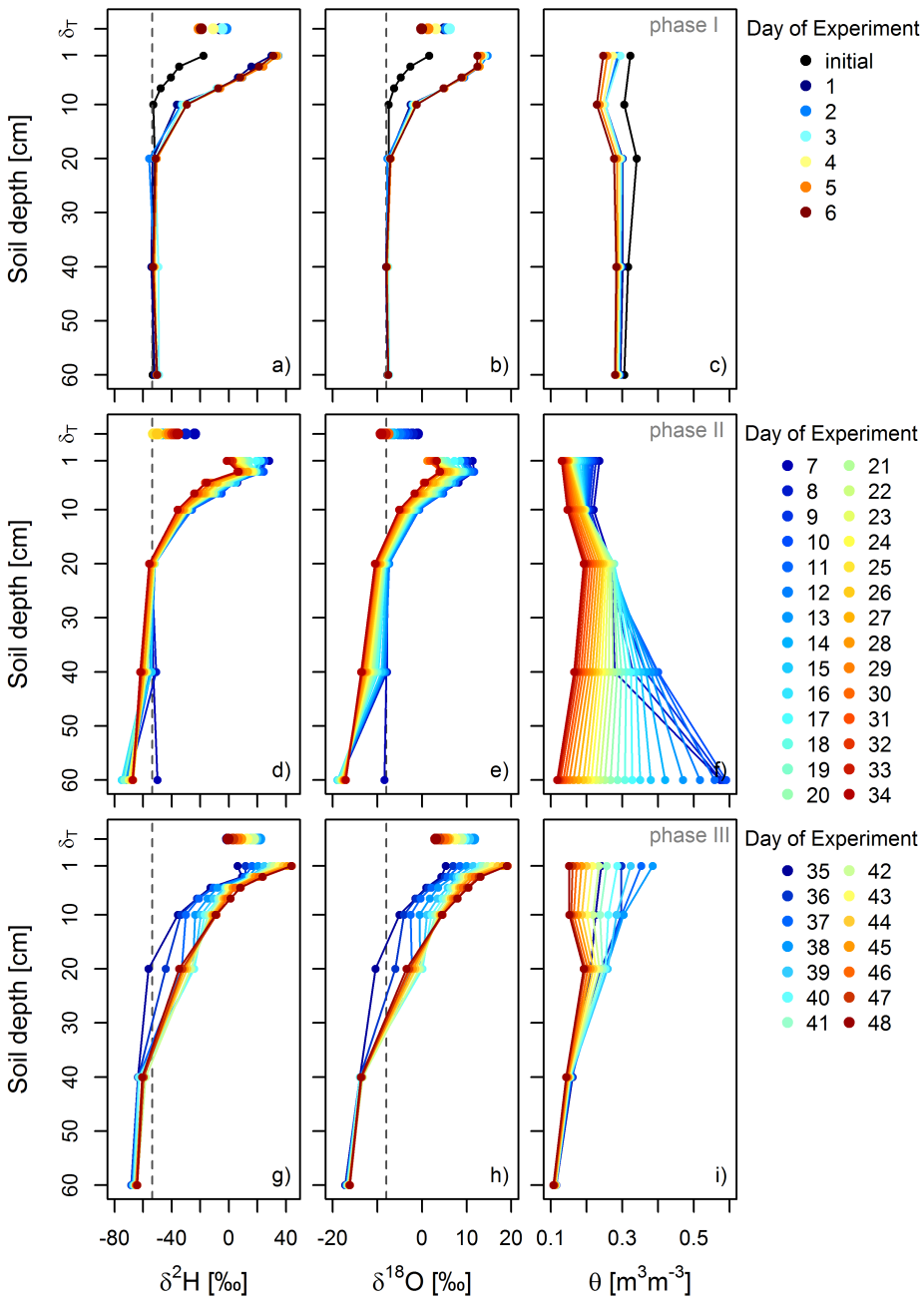
Fig. S2 Temporal evolution of root water uptake fractions without excluding soil water sources prior to modeling

This article is protected by copyright. All rights reserved

section	DoE	1 cm	3 cm	5 cm	7 cm	10 cm	20 cm	40 cm	60 cm
I	1	22 (0-51)	16 (0-50)	19 (0-74)	11 (0-47)	8 (0-41)	7 (0-34)	9 (0-33)	9 (0-35)
	2	20 (0-50)	24 (0-55)	19 (0-57)	5 (0-45)	8 (0-39)	9 (0-31)	7 (0-32)	9 (0-32)
	3	22 (0-57)	20 (0-57)	19 (0-56)	13 (0-52)	6 (0-41)	9 (0-31)	6 (0-33)	6 (0-31)
	4	15 (0-42)	15 (0-42)	13 (0-48)	14 (0-49)	16 (0-42)	7 (0-38)	11 (0-37)	11 (0-38)
	5	6 (0-32)	8 (0-36)	14 (0-42)	18 (0-48)	9 (0-56)	17 (0-47)	15 (0-42)	14 (0-49)
	6	14 (0-37)	8 (0-36)	6 (0-44)	8 (0-43)	12 (0-45)	18 (0-47)	19 (0-49)	15 (0-46)
II	7	14 (0-31)	4 (0-35)	12 (0-42)	3 (0-44)	13 (0-43)	17 (0-48)	19 (0-44)	17 (0-43)
	8	7 (0-35)	10 (0-32)	6 (0-42)	12 (0-45)	16 (0-53)	17 (0-58)	18 (0-53)	14 (0-37)
	9	6 (0-32)	7 (0-32)	4 (0-36)	15 (0-50)	15 (0-52)	20 (0-68)	19 (0-54)	15 (0-42)
	10	5 (0-34)	6 (0-31)	7 (0-38)	8 (0-42)	4 (0-50)	22 (0-63)	22 (0-64)	24 (0-46)
	11	3 (0-31)	8 (0-31)	7 (0-37)	6 (0-41)	6 (0-56)	23 (0-78)	24 (0-72)	24 (0-57)
	12	6 (0-32)	5 (0-37)	6 (0-34)	6 (0-39)	0 (0-52)	22 (0-70)	26 (0-66)	28 (0-61)
	13	5 (0-32)	5 (0-26)	5 (0-30)	7 (0-35)	5 (0-49)	22 (0-78)	24 (0-74)	27 (0-60)
	14	4 (0-29)	5 (0-24)	7 (0-33)	7 (0-37)	5 (0-53)	24 (0-77)	24 (0-74)	25 (0-56)
	15	4 (0-29)	7 (0-23)	6 (0-32)	7 (0-34)	2 (0-48)	24 (0-74)	24 (0-71)	26 (0-61)
	16	5 (0-26)	4 (0-24)	3 (0-28)	6 (0-37)	8 (0-52)	25 (0-67)	15 (0-74)	33 (0-55)
	17	3 (0-30)	5 (0-31)	6 (0-29)	5 (0-37)	4 (0-44)	25 (0-72)	22 (0-79)	30 (0-62)
	18	NA	NA	NA	NA	NA	NA	NA	NA
	19	NA	NA	NA	NA	NA	NA	NA	NA
	20	NA	NA	NA	NA	NA	NA	NA	NA
	21	NA	NA	NA	NA	NA	NA	NA	NA
	22	NA	NA	NA	NA	NA	NA	NA	NA
	23	7 (0-35)	2 (0-30)	4 (0-31)	5 (0-34)	6 (0-42)	21 (0-69)	21 (0-69)	34 (0-62)
	24	3 (0-29)	5 (0-26)	7 (0-33)	6 (0-41)	6 (0-47)	18 (0-70)	24 (0-76)	31 (0-64)
	25	7 (0-44)	4 (0-31)	5 (0-34)	5 (0-35)	7 (0-44)	20 (0-71)	24 (0-75)	28 (0-62)
	26	3 (0-36)	4 (0-31)	4 (0-34)	3 (0-37)	4 (0-47)	21 (0-74)	32 (0-73)	29 (0-62)
	27	8 (0-31)	3 (0-30)	5 (0-36)	7 (0-36)	8 (0-48)	23 (0-62)	24 (0-65)	23 (0-56)
	28	0 (0-0)	6 (0-33)	5 (0-39)	12 (0-45)	18 (0-54)	18 (0-58)	21 (0-62)	21 (0-47)
	29	0 (0-0)	13 (0-30)	8 (0-42)	6 (0-47)	14 (0-49)	20 (0-58)	21 (0-55)	18 (0-48)
	30	0 (0-0)	0 (0-0)	28 (0-47)	18 (0-58)	17 (0-71)	18 (0-66)	19 (0-58)	0 (0-0)
	31	0 (0-0)	0 (0-0)	20 (0-51)	15 (0-67)	22 (0-74)	19 (0-80)	24 (0-65)	0 (0-0)
	32	0 (0-0)	0 (0-0)	0 (0-0)	29 (0-67)	25 (0-87)	24 (0-78)	22 (0-77)	0 (0-0)
	33	0 (0-0)	0 (0-0)	0 (0-0)	0 (0-0)	65 (1-98)	18 (0-91)	18 (0-97)	0 (0-0)
	34	0 (0-0)	0 (0-0)	0 (0-0)	0 (0-0)	0 (0-0)	97 (0-100)	3 (0-100)	0 (0-0)
III	35	38 (0-87)	36 (0-81)	9 (0-66)	3 (0-53)	6 (0-43)	4 (0-42)	4 (0-38)	0 (0-0)
	36	24 (0-83)	21 (0-72)	21 (0-55)	22 (0-60)	4 (0-49)	3 (0-56)	4 (0-49)	0 (0-0)
	37	24 (0-73)	21 (0-64)	17 (0-57)	22 (0-52)	3 (0-49)	9 (0-51)	5 (0-45)	0 (0-0)
	38	22 (0-75)	23 (0-69)	17 (0-50)	17 (0-53)	14 (0-52)	2 (0-49)	4 (0-44)	0 (0-0)
	39	31 (0-90)	10 (0-58)	10 (0-58)	11 (0-61)	13 (0-53)	15 (0-55)	11 (0-41)	0 (0-0)
	40	63 (0-81)	16 (0-68)	4 (0-56)	5 (0-43)	5 (0-45)	4 (0-36)	3 (0-38)	0 (0-0)
	41	44 (0-78)	28 (0-78)	7 (0-58)	6 (0-49)	6 (0-47)	4 (0-44)	6 (0-29)	0 (0-0)
	42	36 (0-76)	24 (0-77)	8 (0-54)	7 (0-54)	6 (0-57)	9 (0-44)	10 (0-42)	0 (0-0)
	43	30 (0-67)	25 (0-71)	12 (0-57)	11 (0-53)	7 (0-50)	7 (0-36)	8 (0-33)	0 (0-0)
	44	21 (0-59)	21 (0-67)	18 (0-70)	19 (0-50)	9 (0-50)	7 (0-46)	4 (0-30)	0 (0-0)
	45	23 (0-52)	19 (0-53)	19 (0-58)	14 (0-54)	13 (0-52)	4 (0-49)	7 (0-34)	0 (0-0)
	46	15 (0-46)	21 (0-58)	12 (0-62)	18 (0-66)	18 (0-59)	15 (0-53)	0 (0-0)	0 (0-0)
	47	4 (0-45)	20 (0-51)	21 (0-60)	14 (0-64)	20 (0-64)	21 (0-66)	0 (0-0)	0 (0-0)
	48	6 (0-47)	6 (0-59)	13 (0-76)	28 (0-66)	20 (0-78)	27 (0-64)	0 (0-0)	0 (0-0)

NA, not available

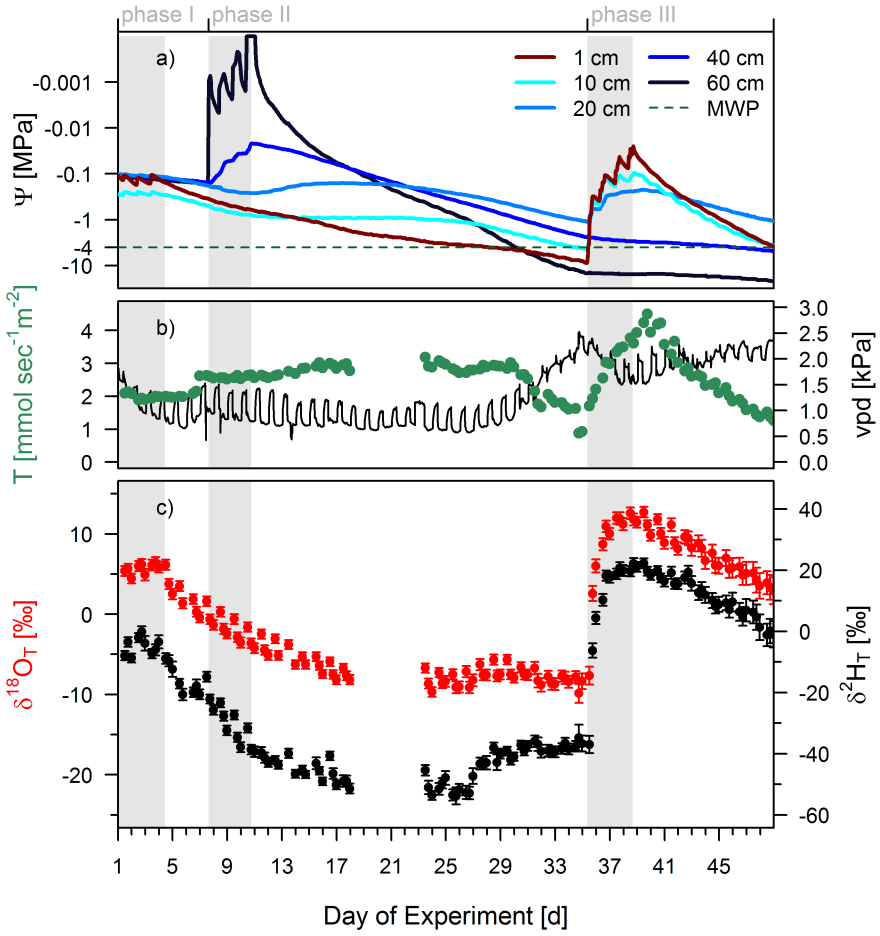
Accepted Article



nph_16352_f1.tiff

This article is protected by copyright. All rights reserved

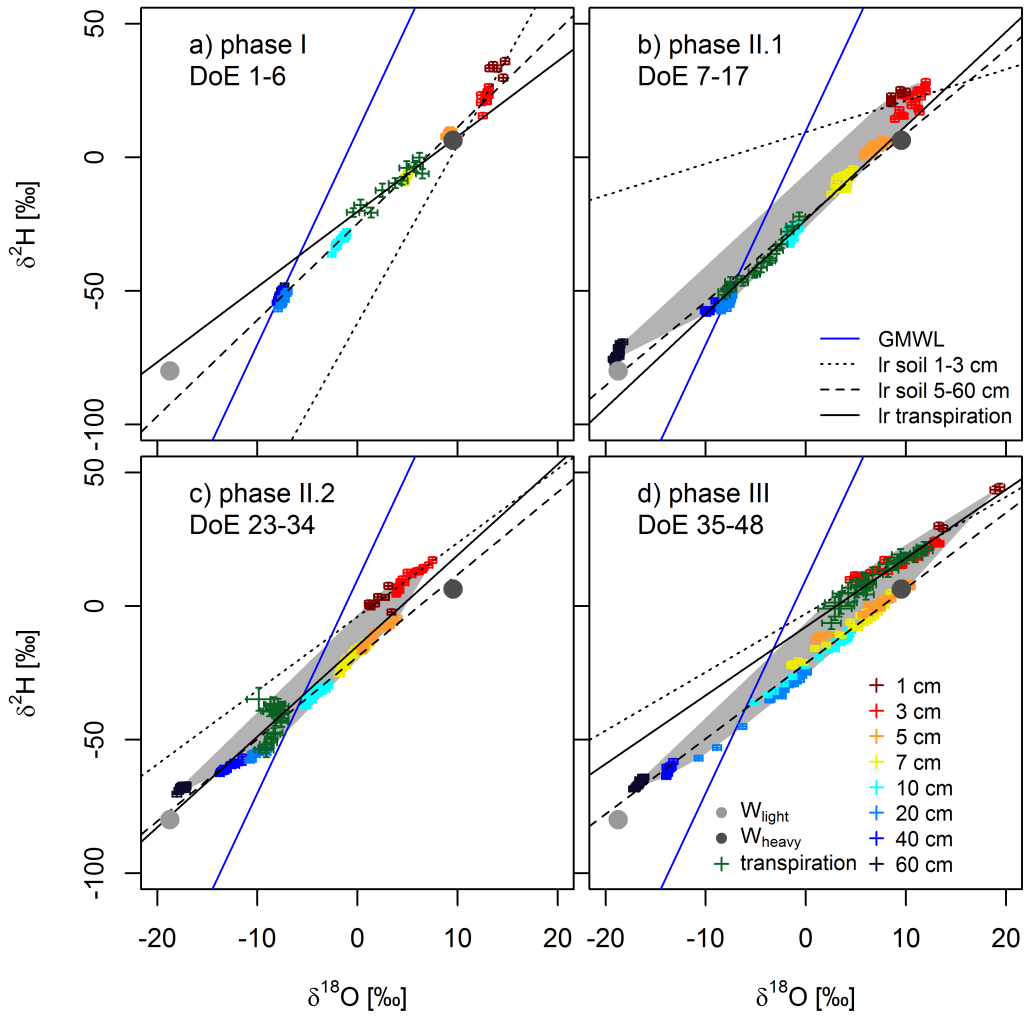
Accepted Article



nph_16352_f2.tiff

This article is protected by copyright. All rights reserved

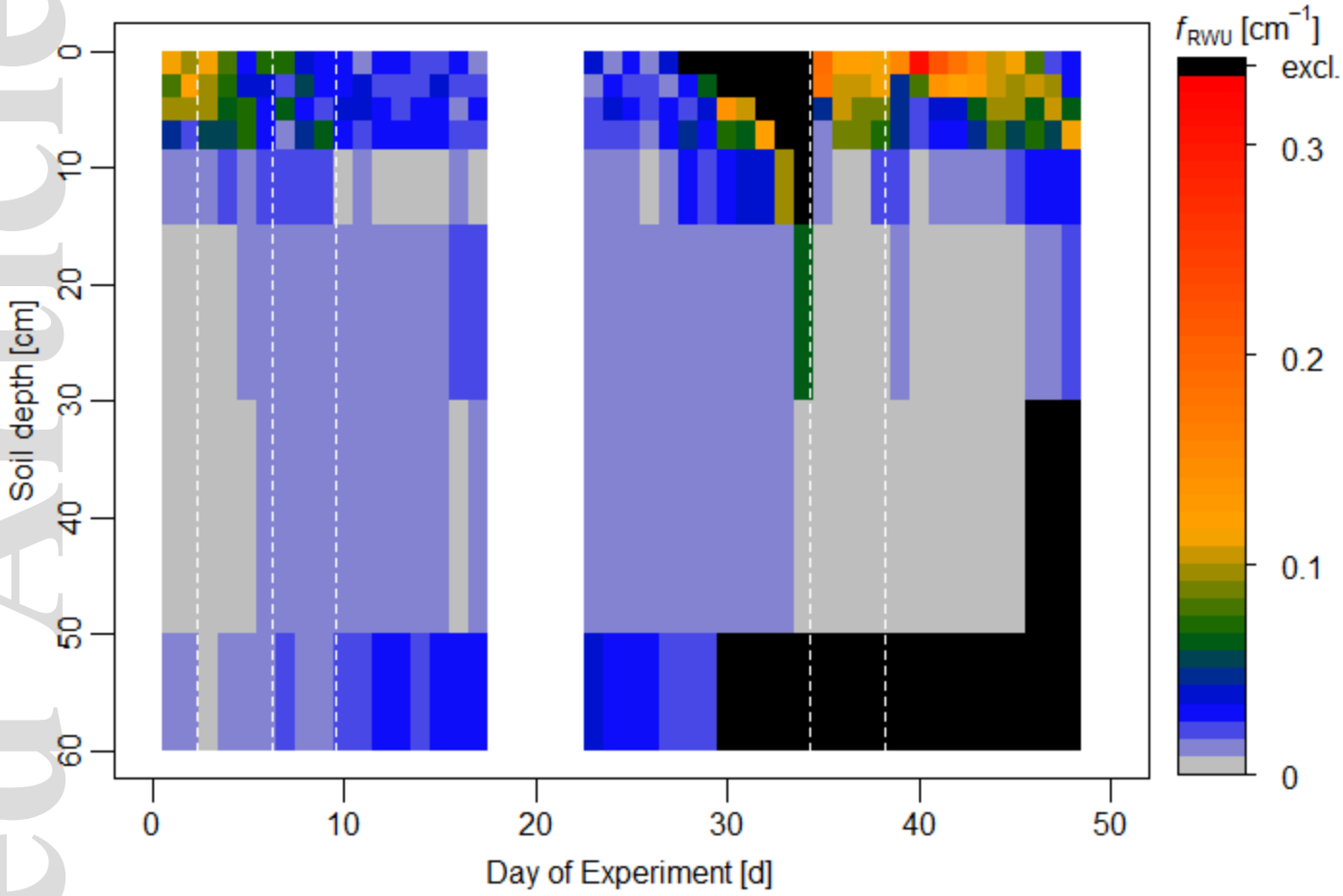
Accepted Article



nph_16352_f3.tiff

This article is protected by copyright. All rights reserved

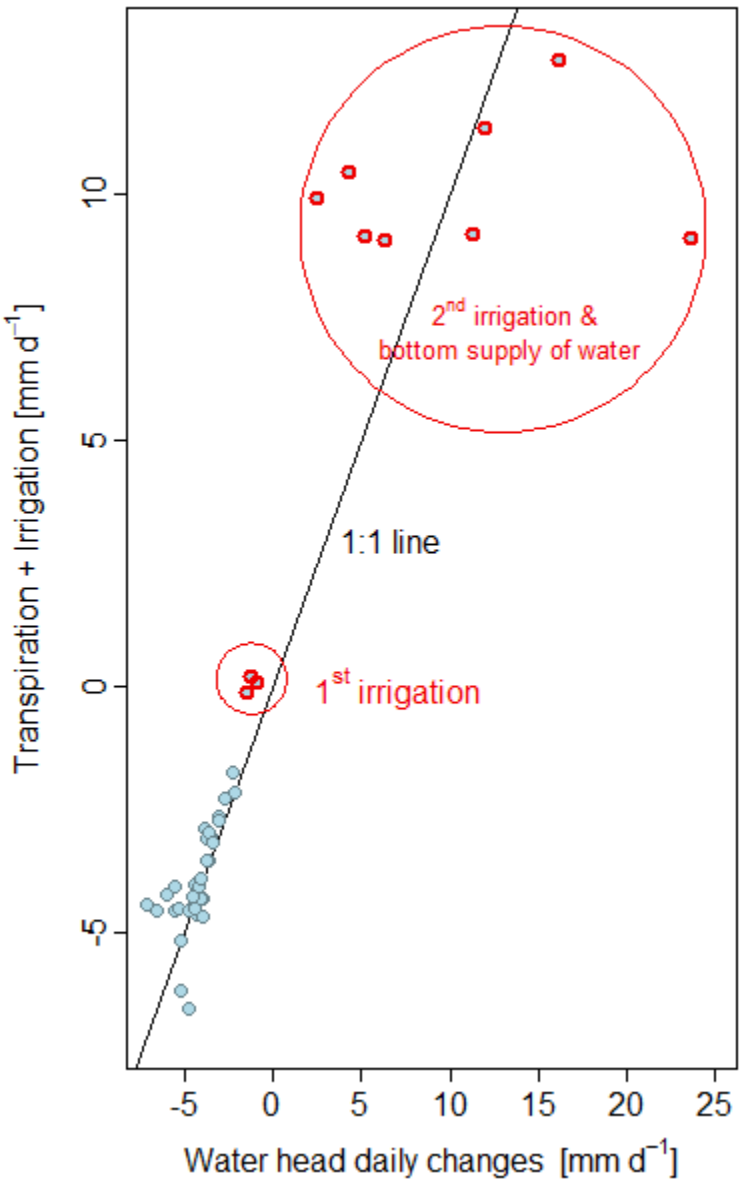
Accepted Article



nph_16352_f4.tiff

This article is protected by copyright. All rights reserved

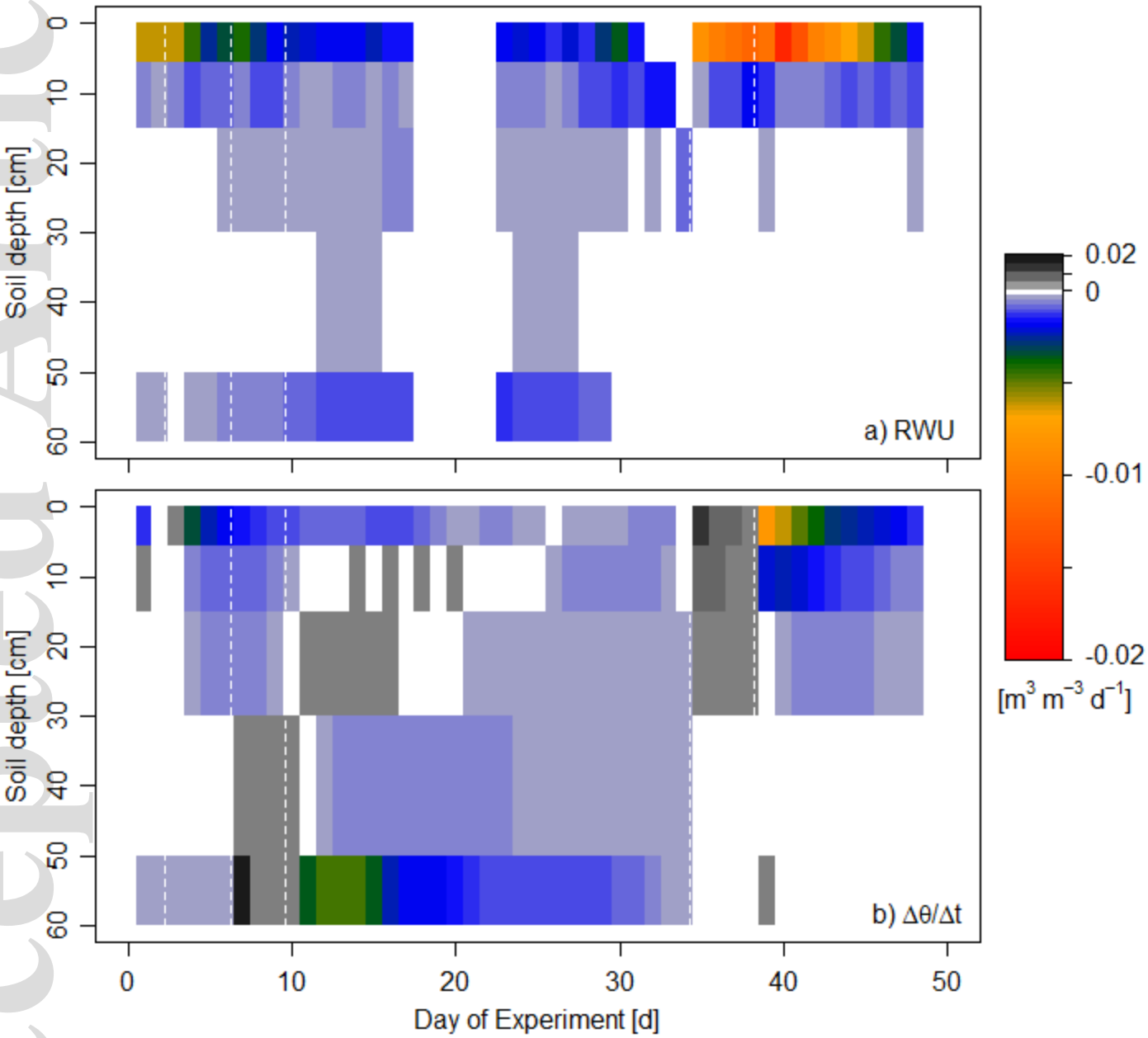
Accepted Article



nph_16352_f5.tiff

This article is protected by copyright. All rights reserved

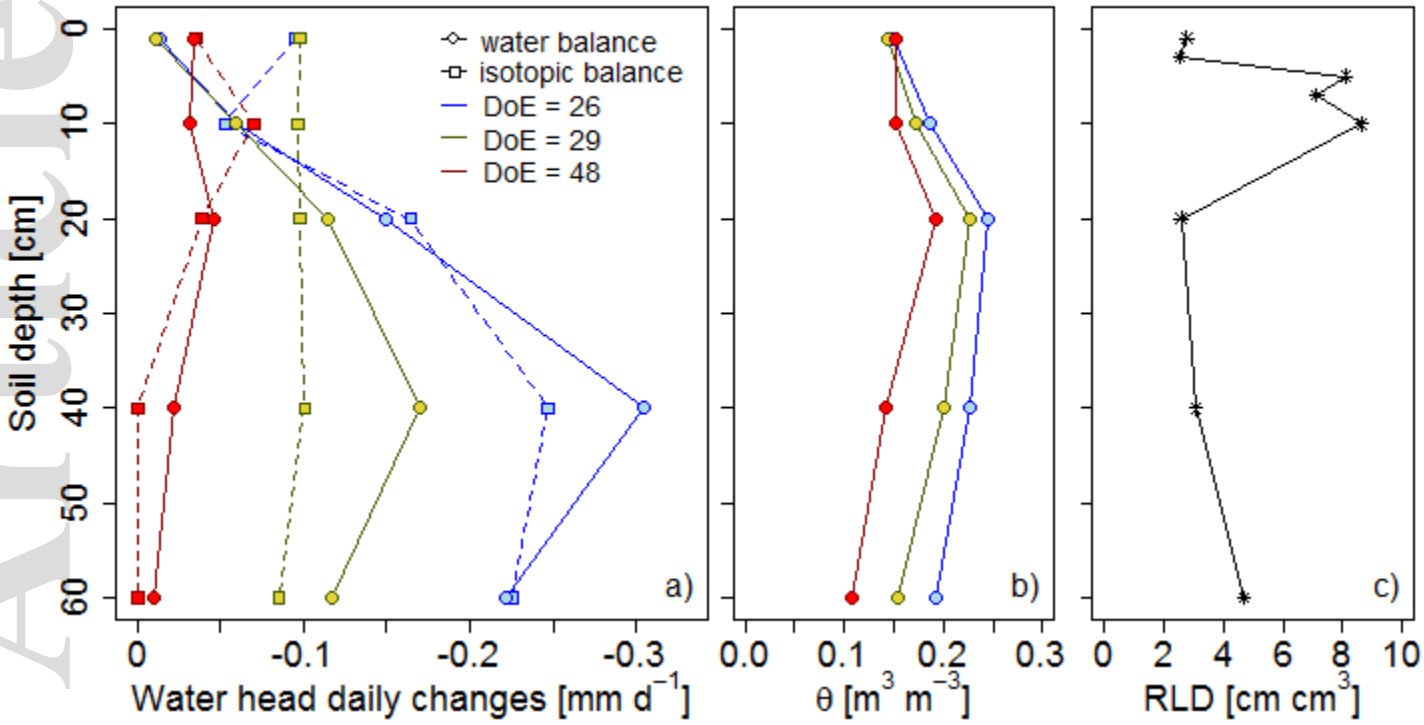
Accepted Article



nph_16352_f6.tiff

This article is protected by copyright. All rights reserved

Accepted Article



nph_16352_f7.tiff

This article is protected by copyright. All rights reserved